Glial Cell Reactivity in a Porcine Model of Retinal Detachment

Ianors Iandiev,[1,2] *Ortrud Uckermann,*[1,3] *Thomas Pannicke,*[1] *Antje Wurm,*[1] *Solveig Tenckhoff,*[2] *Uta-Carolin Pietsch,*[4] *Andreas Reichenbach,*[1] *Peter Wiedemann,*[2] *Andreas Bringmann,*[2] *and Susann Uhlmann*[2]

Purpose. Detachment of the neural retina from the pigment epithelium causes, in addition to photoreceptor deconstruction and neuronal cell remodeling, an activation of glial cells. It has been suggested that gliosis contributes to the impaired recovery of vision after reattachment surgery that may involve both formerly detached and nondetached retinal areas. Müller and microglial cell reactivity was monitored in a porcine model of rhegmatogenous retinal detachment, to determine whether gliosis is present in detached and nondetached retinal areas.

Methods. Local detachment was created in the eyes of adult pigs by subretinal application of hyaluronate. Retinal slices were immunostained against glial intermediate filaments and K^+ and water channel proteins (aquaporin-4, Kir4.1, Kir2.1), and P2Y receptor proteins. In retinal wholemounts, adenosine 5′-triphosphate (ATP)-induced intracellular Ca^{2+} responses of Müller cells were recorded, and microglial and immune cells were labeled with *Griffonia simplicifolia* agglutinin isolectin I-B_4. K^+ currents were recorded from isolated Müller cells.

Results. At 3 and 7 days after surgery, Müller cells in detached retinas showed a pronounced gliosis, as revealed by the increased expression of the intermediate filaments glial fibrillary acidic protein and vimentin, by the decrease of Kir4.1 immunoreactivity and of the whole-cell K^+ currents, and by the increased incidence of cells that showed Ca^{2+} responses on stimulation of purinergic (P)2 receptors by ATP. By contrast, the immunohistochemical expression of Kir2.1 and aquaporin-4 were not altered after detachment. The increase in the expression of intermediate filaments, the decrease of the whole-cell K^+ currents and of the Kir4.1 immunolabeling, and the increase in the Ca^{2+} responsiveness of Müller cells were also observed in attached retinal areas surrounding the focal detachment. The density of microglial-immune cells at the inner surface of the retinas increased in both detached and nondetached retinal areas. The immunoreactivities for $P2Y_1$ and $P2Y_2$ receptor proteins apparently increased only in detached areas.

Conclusions. Reactive responses of Müller and microglial cells are not restricted to detached retinal areas but are also observed in nondetached regions of the porcine retina. The gliosis in the nondetached retina may reflect, or may contribute to, neuronal degeneration that may explain the impaired recovery of vision observed in human subjects after retinal reattachment surgery. (*Invest Ophthalmol Vis Sci.* 2006;47: 2161–2171) DOI:10.1167/iovs.05-0595

Experimental detachment of the neural retina from the pigment epithelium causes complex alterations and remodeling of the retinal tissue.[1] In addition to the initial damage to the outer segments and the apoptotic death of some photoreceptor cells,[2,3] there are morphologic and biochemical alterations of the inner retinal neurons,[4–6] as well as a fast activation of pigment epithelial cells and macro- and microglial cells.[7–11] The activation of glial cells in the detached retina begins within minutes of detachment and proceeds during the first hours and days after creation of a detachment.[8,9,11] The gliosis of Müller cells (the predominant macroglial cells in the retina) is characterized by an upregulation of the immunoreactivity for the intermediate filament constituents vimentin and glial fibrillary acidic protein (GFAP), by cellular hypertrophy and by the development of subretinal fibrosis due to the outgrowth of Müller cell processes.[9,12–14] These morphologic markers of Müller cell gliosis are associated with distinct physiological alterations; among others, the Müller cells downregulate the expression of proteins that are involved in homeostatic functions and in glioneuronal interactions, such as glutamine synthetase, cellular-retinaldehyde-binding protein, and carbonic anhydrase.[7,15] In a rabbit model of rhegmatogenous retinal detachment, we found that Müller cells also downregulate the K^+ conductance of their plasma membranes and upregulate their intracellular Ca^{2+} responsiveness on stimulation of distinct receptors such as purinergic P2Y receptors.[9,11] Normally, the K^+ channels of Müller cells are implicated in the clearance of neuronally released excess K^+ from the retinal tissue,[16] and it has been suggested that the downregulation of functional K^+ channels in gliotic Müller cells contributes to neuronal degeneration after detachment, because an impaired retinal K^+ homeostasis may favor neuronal hyperexcitation and glutamate excitotoxicity.[9]

Reactive gliosis on detachment may be a clinically significant limiting factor in the recovery of vision after reattachment.[12,17,18] The hypertrophied and proliferating glial cells fill the spaces left by dying neurons and degenerated axons, synapses, and photoreceptor segments. The subretinal fibrosis inhibits the regeneration of outer segments,[12] and the hypertrophied side branches of Müller cells that grow into the plexiform layers may limit the reformation of disconnected synaptic contacts.[19] It has been proposed that attempts to

From the [1]Paul Flechsig Institute of Brain Research; the [2]Department of Ophthalmology and Eye Clinic; the [3]Interdisziplinäres Zentrum für Klinische Forschung (IZKF); and the [4]Klinik für Anästhesie und Intensivmedizin, University of Leipzig Medical Faculty, Leipzig, Germany.

Supported by Project C21 of the IZKF at the Faculty of Medicine of the University of Leipzig, the Hochschulwissenschaftsprogrammes (HWP) of the Sächsisches Ministerium für Wissenschaft und Kunst (SMWK), and Grant Br 1249/2-1, GRK 1097/1 from the Deutsche Forschungsgemeinschaft (DFG).

Submitted for publication May 13, 2005; revised September 13, 2005, and January 11, 2006; accepted March 13, 2006.

Disclosure: **I. Iandiev**, None; **O. Uckermann**, None; **T. Pannicke**, None; **A. Wurm**, None; **S. Tenckhoff**, None; **U.-C. Pietsch**, None; **A. Reichenbach**, None; **P. Wiedemann**, None; **A. Bringmann**, None; and **S. Uhlmann**, None

The publication costs of this article were defrayed in part by page charge payment. This article must therefore be marked "*advertisement*" in accordance with 18 U.S.C. §1734 solely to indicate this fact.

Corresponding author: Susann Uhlmann, MD, Department of Ophthalmology and Eye Clinic, University of Leipzig Medical Faculty, Liebigstrasse 10-14, D-04103 Leipzig, Germany; scos@medizin.uni-leipzig.de.

reduce Müller cell gliosis may inhibit retinal degeneration and support neuroregeneration after reattachment.[17,18]

At present, the only effective treatment of retinal detachment is surgery. However, an early and ophthalmoscopically successful retinal reattachment often fails to restore the normal visual capabilities,[20,21] and experimental reattachment does not completely recover the photoreceptor cell layer.[12,22] Even in cases of successful reattachment surgery, patients often describe permanent defects in color vision, and a decline in visual acuity.[23,24] Moreover, after retinal reattachment in cases of local detachment, functional defects were observed also in areas of the visual field that correspond to retinal regions that had not been detached,[25] and the macular function was also found to be depressed in cases of purely peripheral detachment.[20,26] These observations in human subjects indicate that, in addition to the detached retinal areas, the surrounding nondetached retina may undergo distinct reactive changes.

Previously, we described fast physiological alterations of reactive Müller cells in the detached retina of the rabbit.[9,11] However, hypoxia, due to the increase in the distance between the neural retina and the choroid, is one main causative factor of photoreceptor degeneration and glial cell activation in the detached retina.[3,7] Thus, the physiological alterations of reactive Müller cells in the detached avascular retina of the rabbit (entirely depending on choroidal blood supply) may not be representative of detachment of the human retina, which is well vascularized. One purpose of the present study was therefore to reveal whether the physiological alterations of Müller cells on experimental detachment, previously described in the avascular retina of the rabbit, can be also observed in a vascularized retina. A porcine model of rhegmatogenous retinal detachment was used for this purpose. The second purpose was to investigate whether in this model, the gliosis on detachment is restricted to detached retinal areas or whether there are also gliotic alterations in nondetached retinal areas in the neighborhood of local detachment. In addition, we wanted to investigate whether gliotic alterations are associated with alterations in the expression of glial K^+ and water channel proteins (i.e., Kir4.1, Kir2.1 and aquaporin-4).[27–29] These channels have been crucially implicated in the maintenance of water and ion homeostasis in the inner retina performed by Müller cells.[29–31]

Materials and Methods

Surgical Procedure

All experiments were performed in accordance with applicable German laws and with the ARVO Statement for the Use of Animals in Ophthalmic and Vision Research. Fourteen young adult domestic white pigs (17–22 kg; both sexes) were used. Twenty-four hours before and after surgery, the food intake of the animals was restricted, with free access to water. Intramuscular azaperon (15 mg/kg; Cilag-Janssen, Neuss, Germany), atropine (0.2 mg/kg; Braun, Melsungen, Germany), and ketamine (3 mg/kg; Ratiopharm, Ulm, Germany) were administered for premedication. The anesthesia was induced with thiopental (8 mg/kg, intravenously; Trapanal; Byk Gulden, Konstanz, Germany) and maintained with isoflurane (Forene; Abbott, Wiesbaden, Germany). Ventilation was assisted using the Julian respirator (Draegerwerk AG; Luebeck, Germany) with an F_iO_2 of 40%. Rhegmatogenous detachment was created in one eye per animal; the other eye served as the nonsurgical control. The pupils of the eyes were dilated by topical tropicamide (1%; Ursapharm, Saarbrücken, Germany) and phenylephrine hydrochloride (5%; Ankerpharm, Rudolstadt, Germany), and a lateral canthotomy was created. Hemostasis was achieved with wet-field cautery. After pars plana sclerotomy, a circumscript vitrectomy was performed in the area of the future detachment, and balanced saline solution (Delta Select, Pfullingen, Germany) was infused into the eye to replace the vitreous. Thin glass micropipettes attached to 250-μL glass syringes (Hamilton, Reno, NV) were used to create a retinal detachment by subretinal injection of saline followed by 0.25% sodium hyaluronate in saline (Healon; Pharmacia & Upjohn, Dübendorf, Switzerland). The retina ventral of the optic nerve head was detached, whereas the retina dorsal of the optic nerve head remained attached. After surgery, gentamicin (5 mg) and dexamethasone (0.5 mg) were injected subconjunctivally. The lateral canthotomy was closed with 5-0 silk sutures, and atropine (1%) eye drops were instilled into the conjunctival sac. After survival times of 3 (n = 5 animals) and 7 days (n = 5), the animals were anesthetized as described, the eyes were excised, and the animals were killed by intravenous T61 (embutramid mebezonium iodide; 0.65 mL/kg body weight; Hoechst, Unterschleissheim, Germany). To investigate whether the surgical procedure per se induces glial cell activation, vitrectomy (without retinal detachment) was performed in four animals, and the retinas and cells were investigated at 3 days after surgery.

Fluorometrical Ca^{2+} Imaging

Wholemounts of isolated retinal pieces (3 mm^2) were placed, with the vitreous surface up in a perfusion chamber and were incubated for 1 hour at room temperature in extracellular solution containing two different calcium-sensitive fluorescence dyes: Fluo-4/AM (final concentration 22 μM) and Fura-Red/AM (final concentration 17 μM; Invitrogen, Eugene, OR). The extracellular solution contained (mM) 110 NaCl, 3 KCl, 2 $CaCl_2$, 1 $MgCl_2$, 1 Na_2HPO_4, 0.25 glutamine, 10 HEPES, 11 glucose, and 25 $NaHCO_3$, adjusted to pH 7.4 with Tris and bubbled with carbogen (95% O_2, 5% CO_2). After the specimens were washed 10 minutes by continuous perfusion of extracellular solution, test substances were added by rapid (10 seconds) changing of the perfusate. Adenosine 5′-triphosphate (ATP; sodium salt) was purchased from Serva Electrophoresis (Heidelberg, Germany). All other substances used were from Sigma-Aldrich (Taufkirchen, Germany). Fluorescence images were recorded with a confocal laser scanning microscope (LSM 510 Meta; Carl Zeiss Meditec, Inc., Oberkochen, Germany). The fluorescence dyes were excited at 488 nm; the emission of Fluo-4 was recorded with a band-pass filter between 505 and 550 nm, and the emission of Fura-Red was recorded with a 650-nm long-pass filter. Images were taken from the ganglion cell-nerve fiber layers of retinal wholemounts every 5 seconds, from an area of 230 × 230 μm.

Immune Cell Labeling

To label microglial and blood-derived immune cells in the nerve fiber layer, acutely isolated retinal wholemounts were exposed to Cy3-tagged *Griffonia simplicifolia* agglutinin (GSA) isolectin I-B_4 for 1 hour at room temperature. The GSA lectin labels D-galactose residues that are expressed at low level by resting microglial cells and at a higher level by activated microglia, as well as by blood-derived immune cells and endothelial cells. The Cy3 fluorescence was recorded with a 543-nm HeNe laser and a 560- to 615-nm band-pass filter. The degree of microglia-immune cell activation was estimated by counting the density of GSA lectin–labeled cells at the vitreous surface (i.e., in the nerve fiber layer) of retinal wholemounts and by determining two morphologic parameters of the cells: (1) the "cross-sectional" area of their somata and (2) the number of primary cell processes (the latter parameter was assessed by counting those processes that directly arose from the soma and which were longer than 10 μm, i.e., the average soma diameter).

Electrophysiological Recordings

Whole-cell patch–clamp recordings were performed with Müller cells acutely isolated in papain and DNase I-containing solutions, as described previously.[9] The cell suspensions were stored in serum-free modified Eagle's medium at 4°C (up to 6 hours) before use. Voltage-clamp records were performed at room temperature (Axopatch 200A amplifier; Axon Instruments, Foster City, CA) and a computer program (ISO-2; MFK, Niedernhausen, Germany). Patch pipettes were pulled

from borosilicate glass (WPI, Sarasota, FL) and had resistances between 4 and 6 MΩ when filled with the intracellular solution that contained (mM) 10 NaCl, 130 KCl, 1 $CaCl_2$, 2 $MgCl_2$, 10 EGTA, and 10 HEPES (pH 7.1). The signals were low-pass filtered at 1, 2, or 6 kHz (eight-pole Bessel filter) and digitized at 5, 10, or 30 kHz, respectively, with a 12-bit A/D converter. The recording chamber was continuously perfused with extracellular solution consisting of (mM) 135 NaCl, 3 KCl, 2 $CaCl_2$, 1 $MgCl_2$, 1 Na_2HPO_4, 10 HEPES, and 11 glucose (pH 7.4). Alterations of the KCl concentration were made by equimolar changes of the NaCl concentration.

To evoke K^+ currents, depolarizing and hyperpolarizing voltage steps of 250-ms duration, with increments of 10 mV, were applied from a holding potential of −80 mV. The membrane capacitance of the cells was measured by the integral of the uncompensated capacitive artifact (filtered at 6 kHz) evoked by a hyperpolarizing voltage step from −80 to −90 mV when Ba^{2+} (1 mM) was present in the bath solution. Membrane potentials were measured in the current-clamp mode. To evaluate the subcellular distribution of the K^+ conductance, a solution containing 50 mM KCl was pressure-ejected for 50 ms onto four different membrane regions of isolated cells. The evoked currents were recorded at a holding potential of −80 mV through a patch pipette at the soma of the cells.

Immunohistochemistry

Isolated retinas were fixed in 4% paraformaldehyde for 2 hours. After several washing steps in buffered saline, the tissue was embedded in saline containing 3% agarose (wt/vol), and 70-μm thick slices were cut by using a vibratome. The slices were incubated in 5% normal goat serum plus 0.3% Triton X-100 in saline for 2 hours at room temperature and, subsequently, in primary antibodies overnight at 4°C. After washing in 1% bovine serum albumin in saline, the secondary antibodies were applied for 2 hours at room temperature. The following antibodies were used: mouse anti-GFAP (1:200; G-A-5 clone; Sigma-Aldrich), mouse anti-vimentin (1:500; V9 clone; Immunotech, France), rabbit anti-Kir4.1 (1:200; Alomone Laboratories, Jerusalem, Israel), rabbit anti-human Kir2.1 (1:200; Sigma-Aldrich), rabbit anti-rat aquaporin-4 (1:200; Sigma-Aldrich), rabbit anti-$P2Y_1$ (1:100; Alomone), rabbit anti-$P2Y_2$ (1:100; Alomone), rabbit anti-$P2Y_4$ (1:100; Alomone), Cy3-conjugated goat anti-rabbit IgG (1:400; Dianova, Hamburg, Germany), and Cy2-coupled goat anti-mouse IgG (1:200; Dianova). The lack of unspecific staining was proven by negative controls omitting the primary antibodies (not shown). Images were recorded with the confocal laser scanning microscope (LSM 510 Meta; Carl Zeiss Meditec) in single planes. Excitation and emission settings were held constant for all images acquired. The expression levels of immunoreactivities were semiquantified using the image analysis software of the microscope, with detection levels held constant for all slices investigated.

Western Blot Analysis

The retinas were isolated and homogenized in RIPA buffer in the presence of protease inhibitors. The homogenates were centrifuged at 13,000*g* for 10 minutes at 4°C. Protein concentration was determined using the Bradford method. Equal amounts of protein were separated on 12% SDS polyacrylamide gel, transferred to nitrocellulose, and the blots were incubated with anti-Kir4.1 (1:400) for 2 hours at room temperature. Membranes were washed, incubated with alkaline phosphatase conjugate anti-rabbit IgG secondary antibody (1:5000; Sigma-Aldrich-Aldrich) for 1 hour at room temperature, and developed with alkaline phosphatase development tablets (Sigma-Aldrich-Aldrich). The blot shown (see Fig. 6) is representative of results in three independent experiments.

Real-Time PCR

Retinal tissues from two animals were pooled and homogenized (Ultraturrax device; IKA, Staufen, Germany). The total RNA was extracted (RNeasy Mini Kit; Qiagen, Hilden, Germany) and treated with DNase I (Roche, Mannheim, Germany). cDNA was synthesized from 1 μg total RNA (RevertAid H Minus First Strand cDNA Synthesis Kit; Fermentas, St. Leon-Roth, Germany). Real-time PCR was performed (Single-Color Real-Time PCR Detection System; Bio-Rad, Munich, Germany). The PCR solution contained 1 μL cDNA, specific primer set (1 μM each), and 10 μL of nucleic acid stain (QuantiTect SYBR Green PCR Kit; Qiagen) in a final volume of 20 μL. The PCR parameters were initial denaturation and enzyme activation (1 cycle at 95°C for 15 minutes); denaturation, amplification, and quantification (45 cycles at 95°C for 30 seconds, 60°C for 30 seconds, and 72°C for one minute); and a melting curve, 55°C with the temperature gradually increased (0.5°C) up to 95°C. The amplified samples were analyzed by standard agarose gel electrophoresis. The mRNA expression was normalized to the levels of β-actin mRNA. The following primer pairs were used: Kir4.1 (GenBank accession no. AY843528), sense 5′-CAAGGACCTGTGGACAACCT-3′, anti-sense 5′-AATGGTGGTCTGGGATTCAA-3′, producing a 232-bp amplicon; β-actin (accession no. NM_031144), sense 5′-GCGCTCGTCGTCGACAACGG-3′, anti-sense 5′-GTGTGGTGCCAAATCTTCTCC-3′, producing a 248-bp amplicon.

Data Analysis

To investigate whether there is a gradient of glial cell reactivity within the attached tissue, we determined distinct parameters in three different regions in focally detached retinas: in the detached retina, in attached retinal areas near the detachment (peridetached tissue), and at a 10- to 15-mm distance from the edge of the detached retina. The electrophysiological data were not leak-subtracted and were not corrected for liquid junction potentials because they did not exceed 3 mV. The amplitudes of the steady state whole-cell currents were measured at the end of 250-ms voltage steps, and the amplitudes of the inwardly directed K^+ currents were estimated at the voltage step from −80 to −140 mV. The incidence of Müller cells that showed calcium responses was estimated using a procedure described previously.[32] As a rough estimate of the activation-infiltration of microglial and blood-derived immune cells, the number of isolectin-stained cells per unit of retinal surface area (230 × 230 μm) in the nerve fiber layer of the wholemounts was counted manually using the microscope software. Statistical analysis (unpaired Student's *t*-test, Mann-Whitney) was performed on computer (Sigma-Plot program; SPSS, Chicago, IL or Prism; GraphPad Software, San Diego, CA). Data are expressed as the mean ± SEM; *n* represents the number of retinal wholemounts (calcium imaging) and the number of isolated cells investigated (electrophysiological recordings), respectively.

Results

Cell Membrane Capacitance of Isolated Müller Cells

To reveal cellular hypertrophy, the membrane capacitance of acutely isolated Müller cells was measured electrophysiologically as an indicator of the cell membrane area. The membrane capacitance of Müller cells isolated from detached retinas was significantly larger than that of cells from nonsurgical control retinas (Fig. 1). There was apparently a gradient of Müller cell hypertrophy in the attached retina after surgery, with greater cells in the attached tissue immediately adjacent to the focal detachment and smaller cells in the tissue more distant from the detached retina (Fig. 1). Vitrectomy alone (without retinal detachment) evoked no significant ($P > 0.05$) alteration of the cell membrane capacitance (Fig. 1), suggesting that operation procedure per se did not cause Müller cell hypertrophy.

K^+ Currents of Isolated Müller Cells

Examples of whole-cell records of K^+ currents from typical cells isolated from a nonsurgical control retina and from detached and attached retinal areas of an surgical eye at 7 days after surgery, are shown in Figure 2A. Within 3 days after

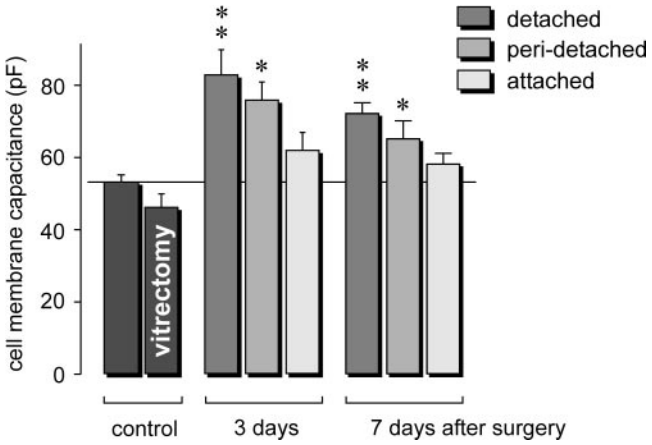

FIGURE 1. Experimental detachment caused hypertrophy of porcine Müller cells. The whole-cell membrane capacitance of acutely isolated cells (which is a relative marker of the cell membrane area) was measured electrophysiologically. The data were determined in cells derived from nonsurgical control eyes, from vitrectomy control eyes, from detached retinas, and from attached retinal areas located in situ near (peridetached) or more distant (10–15 mm) from the detached retina (attached). The vitrectomy control was investigated at 3 days after vitrectomy without creation of detachment. The data were obtained in 9 to 26 cells. Significant differences versus nonsurgical control: $^{*}P < 0.05$; $^{**}P < 0.01$.

surgery, Müller cells isolated from detached retinas strongly decreased the amplitudes of their transmembrane K^+ currents, in the mean by ~75% compared with control (Fig. 2B). The cells isolated from the nondetached tissue of the surgical eyes did not display a significant alteration of the amplitude of their K^+ currents during this time. However, at 7 days of focal detachment, both Müller cell populations investigated (from detached and nondetached retinal areas) displayed a significant downregulation of their K^+ currents, by ~72% and ~58%, respectively (Fig. 2B). Apparently, there was a gradient of changes in cells from the attached retina at 7 days after surgery, with smaller currents in cells isolated from tissue near the detachment compared with cells isolated from tissue more distant to the detachment (Fig. 2C). Cells from vitrectomized control eyes and from nonsurgical control eyes displayed similar current amplitudes (Fig. 2B). The subcellular distribution of the K^+ conductance of Müller cells was tested by applying a high-K^+ solution locally at four distinct membrane regions of isolated cells and measuring the current responses. In Müller cells from nonsurgical control eyes, the relative K^+ conductance was largest at the end foot region of the cells (Fig. 2D). At 7 days after surgery, we observed a general decrease of the local K^+ conductance in Müller cells. Furthermore, the conductance peak at the end foot membrane observed in cells from nonsurgical control retinas was absent in the cells of the surgical eyes; rather, the K^+ conductance was evenly distributed along the cells. The membrane potential of Müller cells significantly decreased in such cell populations that showed a reduction of the K^+ currents (Fig. 2E).

ATP-Evoked Ca^{2+} Responses in Müller Cells

The Ca^{2+} responses of Müller cells were recorded in acutely isolated retinal wholemounts at the plane of the cell end feet. Extracellular application of ATP (10 or 200 μM) evoked transient increases of the intracellular free Ca^{2+} in some Müller cell end feet of nonsurgical control retinas (Fig. 3A). In the mean, ~5% and ~13% of the recorded cell end feet in wholemounts derived from nonsurgical control retinas displayed Ca^{2+} responses on application of 10 and 200 μM ATP, respectively. Wholemounts obtained from detached retinas at 3 or 7 days after surgery displayed a significant increase in the incidence of responding Müller cells when compared with the control (Figs. 3B, 3C). Of note, the increase in the Ca^{2+} responsiveness to 200 μM ATP was apparently transient during detachment, with a significant lower incidence in retinas that were detached for 7 days than after 3-day detachment (Fig. 3C). A similar transient upregulation of Ca^{2+} responsiveness was observed in wholemounts derived from nondetached retinal tissues, with significantly elevated responses at 3 days after surgery (Fig. 3B, 3C). The vitrectomy control displayed no significant alteration of the Ca^{2+} responsiveness of Müller cells when compared to untreated control (Fig. 3C).

Immunoreactivities for Intermediate Filament Proteins

In retinas from nonsurgical control eyes, the strongest immunoreactivity for vimentin was found in the nerve fiber layer (Fig. 4A). In addition, Müller cell fibers within the inner retinal layers displayed staining for vimentin. At 3 (not shown) and 7 days after creation of detachment (Fig. 4A), the vimentin labeling of Müller cells strongly increased in the detached and surrounding attached retinal tissues, with staining of Müller cell fibers in the whole retinal tissue. The immunoreactivity for GFAP was largely restricted to the nerve fiber layer in the nonsurgical control tissue, reflecting the prominent expression of GFAP by retinal astrocytes and Müller cell end feet (Fig. 4D). A few vitreous stem processes of Müller cells were also stained in the inner half. At 3 (not shown) and 7 (Fig. 4D) days after surgery, the expression of GFAP by Müller cells in detached and nondetached retinal areas was strongly increased, with a prominent expression of the filament protein throughout the length of the Müller cell fibers. Semiquantification of the immunoreactivities for GFAP (Figs. 5A, 5B) and vimentin (Fig. 5C) in retinal slices showed increases in the levels in detached and attached retinal areas. The distribution of GFAP (Figs. 4E, 5A, 5B) and vimentin (Fig. 5C) immunoreactivities did not differ between slices from nonsurgical and vitrectomized control eyes, suggesting that vitrectomy per se did not cause an activation of Müller cells.

Immunoreactivities for K^+ Channel Proteins

The predominant K^+ channel subtype expressed by Müller cells is the Kir4.1 channel.[27,29–31] In retinas from nonsurgical control eyes of the pig, the immunoreactivity for Kir4.1 was observed in membranes of Müller cells that surround the retinal vessels, in membranes of Müller cell end feet that abut the inner limiting membrane (ILM), and within the nerve fiber layer (Fig. 4A). In detached retinas obtained at 3 (not shown) or 7 (Fig. 4A) days after surgery, the Kir4.1 immunoreactivity was strongly downregulated in comparison to control retinas. At 7 days after surgery, the perivascular Kir4.1 immunolabel was decreased also in nondetached tissues of surgical eyes when compared with the nonsurgical control, while a significant staining at the ILM remained demonstrable, though at a lower level when compared with the control (Fig. 4A). Semiquantitative evaluation of the Kir4.1 staining within the inner nuclear layer revealed a strong decrease in Kir4.1 protein expression in detached and attached retinal areas at 7 days after surgery (Fig. 5D). Vitrectomy per se did not alter the retinal distribution of Kir4.1 immunoreactivity when compared with retinal slices of nonsurgical control eyes (Figs. 4B, 5D).

Müller cells express different subtypes of K^+ channels.[29] In addition to the Kir4.1 protein, Müller cells of the pig expressed Kir2.1 protein at membrane domains that face the neuropil (Fig. 4C). Apparently, the overall expression of Kir2.1 immu-

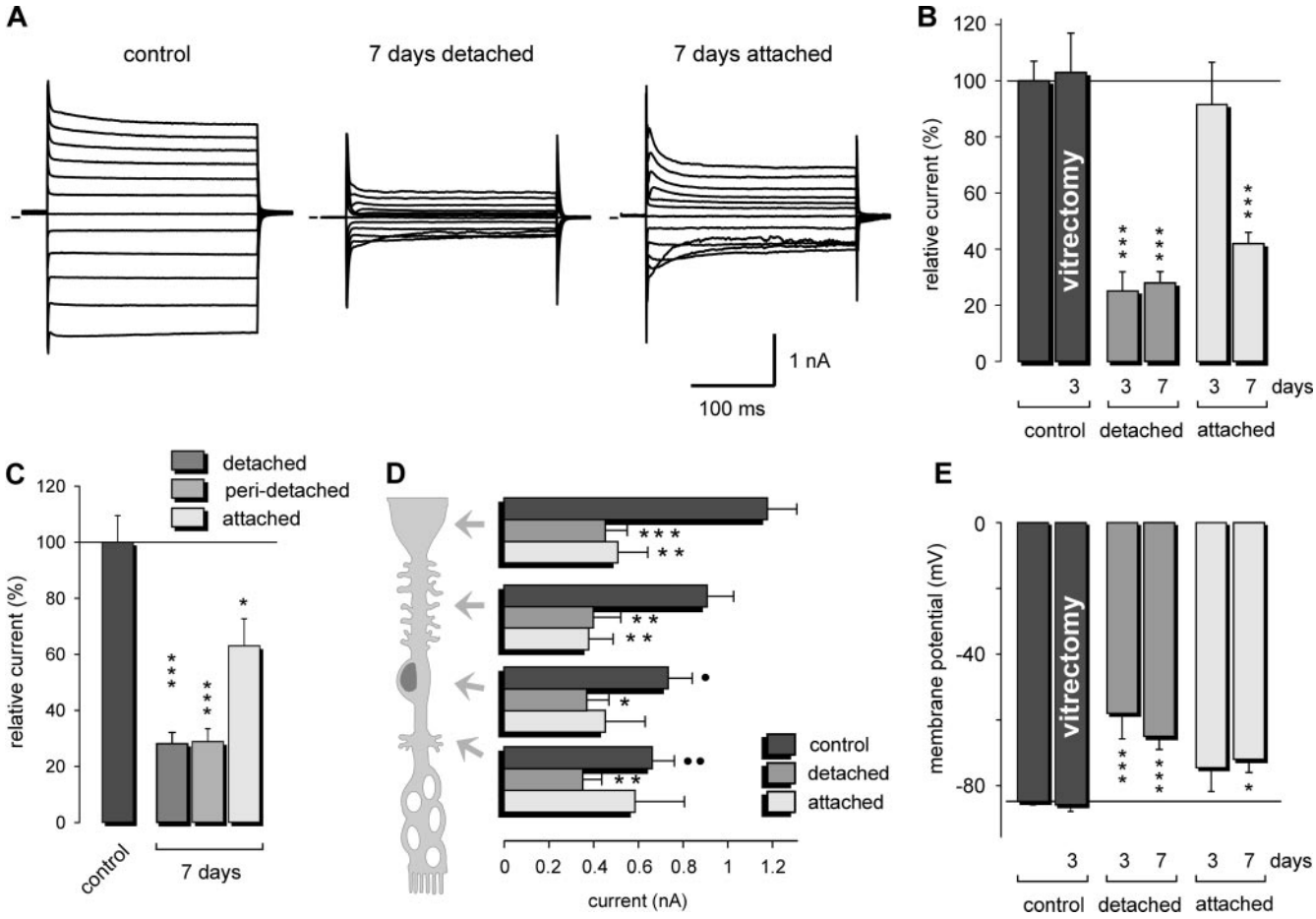

FIGURE 2. Experimental detachment altered the K^+ currents of porcine Müller cells. The cells were isolated from nonsurgical control and detached retinas and from nondetached retinal tissues of surgical eyes and were investigated at 3 and 7 days after surgery. The vitrectomy control was investigated at 3 days after vitrectomy without creation of detachment. (**A**) Examples of typical current records in cells isolated from a control retina and from detached and attached retinal areas of a surgical eye at 7 days after surgery. Voltage steps were applied from a holding potential of −80 mV to de- and hyperpolarizing potentials between −180 and +40 mV (20-mV increments). *Small bars* at the *left* indicate zero-current level. (**B**) The amplitude of the inward currents was measured at the voltage step from −80 to −140 mV and is shown as a percentage of the values obtained in cells from the contralateral nonsurgical control eyes (100%). (**C**) Relative K^+ current amplitude in cells that were isolated from untreated control eyes, detached retinas, and attached retinal areas located in situ near (peridetached) and more distant (10–15 mm) from the detached retina (attached), respectively. (**D**) Subcellular distribution of the K^+ conductance in porcine Müller cells. The inwardly directed K^+ currents were evoked by focal application of a 50-mM K^+ solution onto four different membrane domains (cell end foot, proximal stem process, soma, and distal stem process) and were recorded at the cell soma. (**E**) Membrane potential. Each bar represents values obtained in 12 to 26 cells. Significant differences versus nonsurgical control: $^*P < 0.05$; $^{**}P < 0.01$; $^{***}P < 0.001$. Significant differences versus end foot control: $^{\bullet}P < 0.05$; $^{\bullet\bullet}P < 0.01$.

noreactivity did not decrease in detached (Fig. 4C) and attached (not shown) retinal tissues obtained up to 7 days after surgery.

Gene and Protein Expression of Kir4.1

By using semiquantification, we found a significant downregulation of Kir4.1 immunoreactivity in retinal slices after detachment (Fig. 5D). To determine whether the retinal protein content and gene expression is altered after focal detachment we performed Western blot and PCR investigations. As shown in Figure 6A, the retinal content of Kir4.1 protein was markedly lower in detached and nondetached tissues of surgical eyes compared with control tissue derived from nonsurgical eyes. By using real-time PCR, we found a lower content of mRNA for Kir4.1 in tissues of surgical eyes compared with control tissue. The data suggest that both the gene and protein expression of Kir4.1 is downregulated in Müller cells after detachment.

Immunoreactivity for Aquaporin-4

In the retina, aquaporin-4 is expressed by Müller cells.[28,30] In retinas from nonsurgical control eyes of the pig, immunoreactivity for aquaporin-4 was found in the inner retinal layers, with the most pronounced expression around blood vessels and at the ILM (Fig. 4D). In addition, a diffuse staining for aquaporin-4 was observed in the nerve fiber and ganglion cell layers. In detached and attached retinal tissues obtained at 3 or 7 days after surgery, the overall pattern of aquaporin-4 distribution was not altered in comparison with the control (Fig. 4D).

Immunoreactivities for P2Y Receptors

We showed that the Ca^{2+} responsiveness on ATP (an agonist of purinergic P2 receptors) increased in Müller cells from detached retinas (Figs. 3B, 3C). Therefore, we investigated whether the expression of metabotropic P2Y receptors changed after detachment. In retinas from nonsurgical control eyes of the pig, immunoreactivity for the $P2Y_1$ receptor pro-

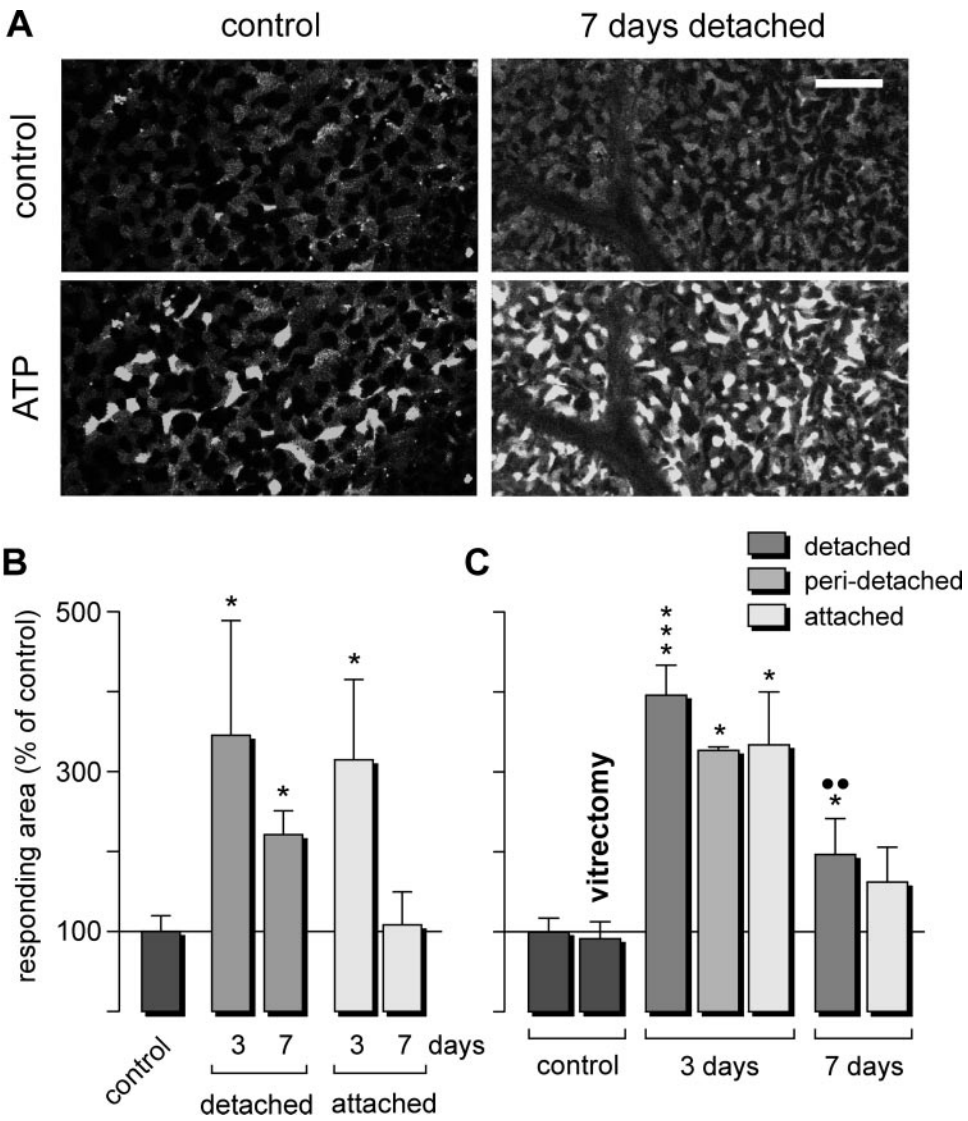

FIGURE 3. Experimental detachment increased Ca^{2+} responsiveness to purinergic receptor stimulation in porcine Müller cells. The Ca^{2+} responses in Müller cell end feet were evoked by bath application of ATP and were recorded in the ganglion cell–nerve fiber layers of acutely isolated retinal wholemounts. (**A**) Examples of Ca^{2+} responses in the ganglion cell layer of wholemounts derived from a control retina and a retina detached for 7 days. The images show the fluorescence of Fluo-4 and were recorded before application of ATP (200 μM) and at the peak Ca^{2+} responses. In the control retina, single end feet of Müller cells showed Ca^{2+} responses, whereas in the detached retina, most of the Müller cell end feet displayed responses. Scale bar, 50 μm. (**B**, **C**) Mean area of Müller cell end feet that showed a Ca^{2+} response on application of 10 μM (**B**) or 200 μM ATP (**C**). In (**C**), the area of responding end feet was determined in the detached retina and in attached retinal areas located in situ near (peridetached) or more distant (10–15 mm) from the detached retina (attached), respectively. The vitrectomy control was determined at 3 days after vitrectomy without creation of detachment. Data are given as the percentage of the mean calcium response in retinas of nonsurgical control eyes (100%). The bars represent values obtained in 3 to 12 wholemounts. Significant differences versus nonsurgical control: $^{*}P < 0.05$; $^{***}P < 0.001$. Significant difference between 3 and 7 days of detachment: $^{\bullet}P < 0.01$.

tein was expressed prominently within the ganglion cell and inner nuclear layers (Fig. 4F). After 7 days of detachment, the expression of $P2Y_1$ immunoreactivity was diffusely upregulated within the retinal tissue and was partially colocalized with vimentin-positive Müller cell fibers (yellow merge signal in Fig. 4F). There was no difference in the expression in the nondetached tissues when compared with the control samples (not shown). Immunoreactivity for the $P2Y_2$ receptor protein was expressed predominantly in the innermost retinal layers, probably by astrocytes and some Müller cell fibers (Fig. 4F). After 7 days of detachment, $P2Y_2$ immunoreactivity was upregulated diffusely throughout the retinal tissue, and there was a partial colocalization of $P2Y_2$ immunoreactivity with vimentin-positive fibers of Müller cells. In the nondetached tissue, in contrast, the staining pattern was unchanged compared with control tissue (not shown). Semiquantification of the expression of $P2Y_2$ immunoreactivity within the outer retina revealed a strong increase of labeling in tissues that were detached for 7 days, whereas attached tissues displayed no alteration compared with the control (Fig. 5E). Immunoreactivity for the $P2Y_4$ receptor protein was expressed in the innermost retinal layers, probably by astrocytes, in the outer plexiform layer, and

FIGURE 4. Experimental detachment in porcine eyes changed the expression of various proteins by glial cells in both detached and nondetached retinal areas. The slices were derived from nonsurgical control retinas, from vitrectomized control retinas, and from detached and attached areas of porcine retinas at 7 days after surgery. The attached tissues were derived from an area located in situ near the detachment (peridetached) or from areas more distant (10–15 mm) from the detachment (attached). (**A**) Immunoreactivities for Kir4.1 (*red*) and vimentin (*green*). (**B**) Immunoreactivity for Kir4.1 in slices from nonsurgical and vitrectomized retinas. (**C**) Immunoreactivity for Kir2.1. (**D**) Immunoreactivities for aquaporin-4 (*red*) and GFAP (*green*). (**E**) Immunoreactivity for GFAP in slices from nonsurgical and vitrectomized retinas. (**F**) Immunoreactivities for $P2Y_1$, $P2Y_2$, and $P2Y_4$ receptor proteins (*red*), respectively. The slices were coimmunostained against vimentin or GFAP (*green*). Coexpression of the proteins yielded a *yellow* merge signal. (**G**) Isolectin staining of retinal slices, marking blood vessels and microglial–immune cells. Cell nuclei were counterstained with Hoechst 33258 (*blue*). (**A**, **D**) *Arrowheads*: inner limiting membrane; *arrows*: perivascular staining. (**F**) *Arrows*: vimentin-positive fibers in the outer retina that were also stained for $P2Y_2$ protein. (**G**) Microglial cell bodies (*arrows*) and processes (*arrowheads*), respectively. Scale bars, 20 μm. GCL, ganglion cell layer; INL, inner nuclear layer; IPL, inner plexiform layer; NFL, nerve fiber layer; ONL, outer nuclear layer.

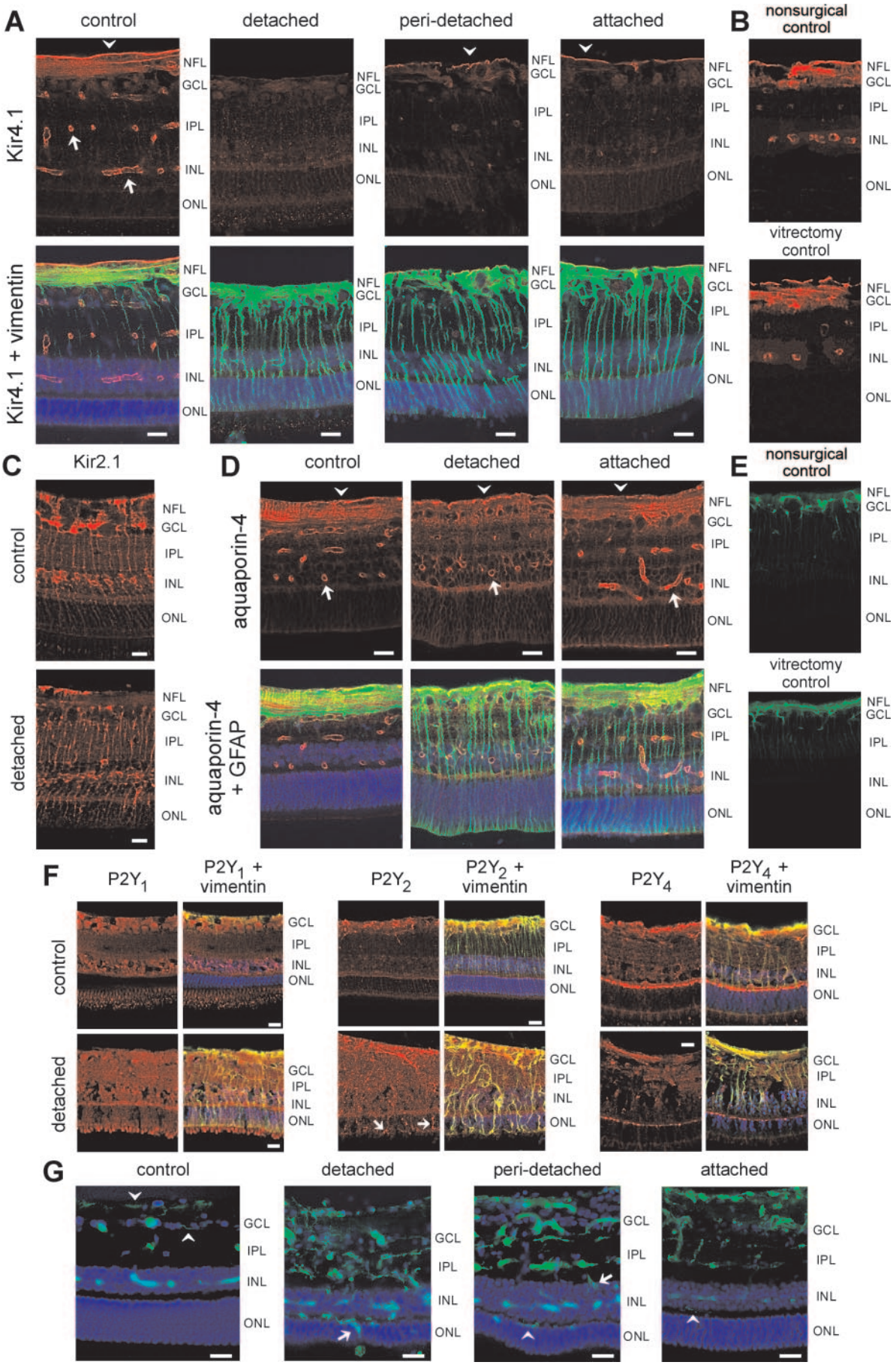

FIGURE 4.

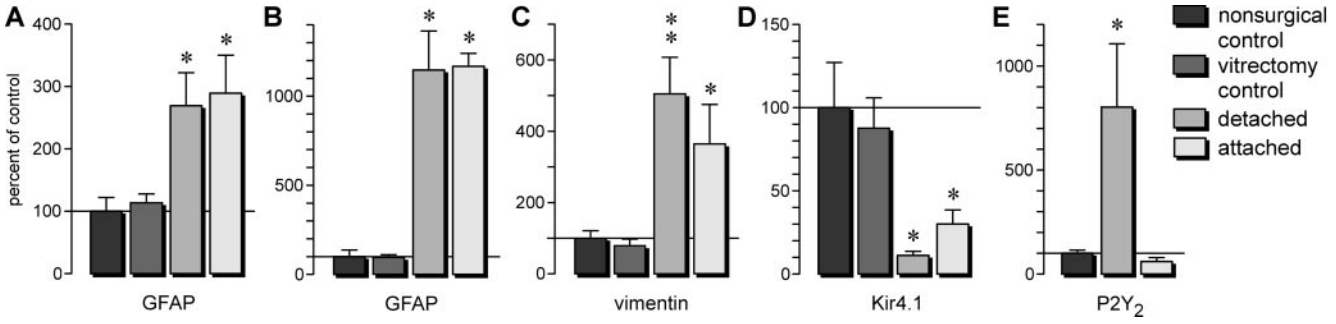

FIGURE 5. Relative expression levels of immunoreactivities for distinct proteins in slices of the pig retina. The slices were derived from nonsurgical control retinas, from vitrectomized control retinas, and from detached and attached areas of porcine retinas at 7 days after surgery. (**A**, **B**) Immunoreactivity for GFAP in the whole retinal slices (**A**) and in the outer nuclear layer (**B**). (**C**) Immunoreactivity for vimentin in the outer nuclear layer, for (**D**) Kir4.1 within the inner nuclear layer, and for (**E**) the $P2Y_2$ receptor protein in the outer retina. Data represent values obtained in 3 to 17 slices from three animals, and are expressed as a percentage of the nonsurgical control (100%). Significant differences versus control: $^*P < 0.05$; $^{**}P < 0.01$.

more diffusely in the inner plexiform layer (Fig. 4F). At 7 days after surgery, there was no apparent difference between the staining patterns of detached and nondetached tissues, and the nonsurgical control.

Microglia–Immune Cell Activation

Experimental focal detachment caused significant increases in the number of isolectin-labeled cells in the nerve fiber layer of retinal wholemounts derived from both detached and attached retinal areas of the surgical eyes (Fig. 7). Apparently, there was a gradient of immune cell density in the nerve fiber layer at 3 and 7 days after creation of detachment, with the highest density of cells in the detached tissue and the lowest density in the more distant attached tissue, although the difference between these areas did not achieve statistical significance ($P > 0.05$; Fig. 7B). Vitrectomy alone (without retinal detachment) evoked a small but significant ($P < 0.05$) increase in immune cell density at 3 days after surgery which was significantly smaller when compared with the cell densities in detached and attached retinal areas (Fig. 7B). The morphology of the isolectin-stained cells displayed no alterations in both detached and attached retinal areas. Microglial cells in nonsurgical control retinas exhibited the typical ramified morphology of resting microglia (Fig. 7A), with relatively small somata (77.7 ± 7.8 μm^2 area in the optical section), a bipolar shape (2.7 ± 0.3 primary processes), and multiple thin and long side branches (not determined). These morphologic parameters did not change significantly after 3 days (soma area: 81.3 ± 10.4 μm^2; number of primary processes: 2.1 ± 0.4) or 7 days (not shown) after surgery.

Degeneration of photoreceptor segments in detached retinas may represent a stimulus that evokes migration of microglial cells within the tissue. We found that migration of isolectin-labeled cells was observed in the detached retina and, to a lower degree, in the attached retina in the neighborhood of a focal detachment. In nonsurgical control retinas, isolectin-labeled processes of microglial cells were restricted to the nerve fiber-ganglion cell layers (Fig. 4G). In retinas that were detached for 7 days, microglial cell bodies were observed to be present in the whole retinal tissue. In attached retinal areas, microglial cell bodies were observed also in the inner plexiform layer and extended single processes to the outer plexiform layer (Fig. 4G).

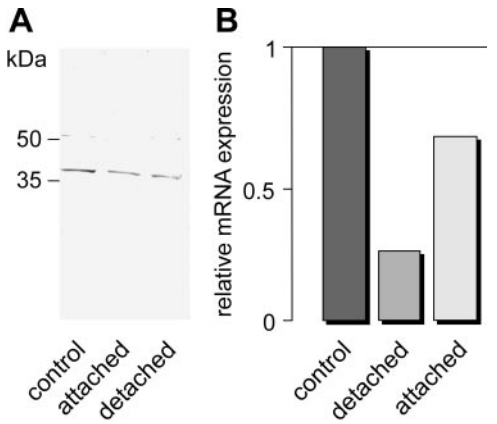

FIGURE 6. Relative retinal expression levels of the Kir4.1 protein and mRNA. (**A**) Western blot analysis was conducted with retinal tissue of one animal at 7 days after surgery. Similar results were obtained in three independent experiments. (**B**) The mRNA expression was determined by real-time PCR in retinal tissue pooled from two animals at 7 days after surgery and was normalized to the levels of mRNA for β-actin.

DISCUSSION

It has been shown that experimental retinal detachment causes a rapid glial cell activation that begins within minutes of detachment and proceeds further during the first hours and days after creation of the detachment.[8,9,11] Using a rabbit model of rhegmatogenous detachment, we previously described not only morphologic and biochemical alterations but also distinct physiological alterations, such as a downregulation of the K^+ conductance and an upregulation of the intracellular Ca^{2+} responsiveness on stimulation of P2Y receptors[9,11] in the reactive Müller cells. However, because hypoxia of the outer retina is one main causative factor of photoreceptor degeneration and glial cell activation in the detached retina,[3,7] it may be argued that detachment causes much more severe glial cell responses in the avascular retina of the rabbit than in a vascularized retina such as the human retina (where the blood supply is not disrupted after detachment). Porcine eyes are similar to human eyes in size, retinal ultrastructure, and circulation.[33,34] In our study, the detached porcine retina displayed similar physiological alterations of Müller cells as the detached retina of the rabbit. Moreover, the present results provide new information regarding the immunohistochemical expression of the glial K^+ and water channel proteins, Kir4.1, Kir2.1, and aquaporin-4, and of P2Y receptors in the detached retina, and regarding gliotic responses in nondetached retinal areas in the neighborhood of local detachment.

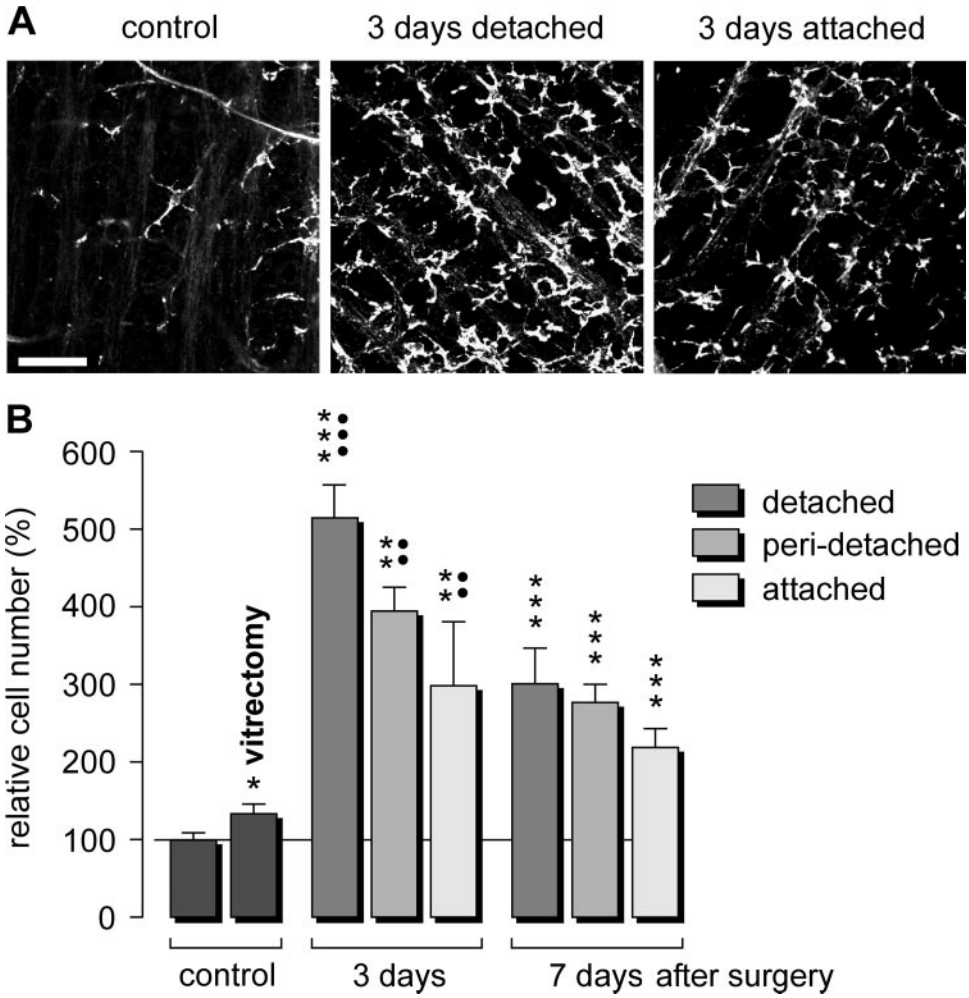

FIGURE 7. Experimental detachment caused an increase in the density of isolectin-labeled microglial/immune cells in the nerve fiber layer of porcine retinas. (**A**) Image records of the vitreous surface (i.e., view onto the nerve fiber layer) of wholemounts derived from an nonsurgical control retina, from a retina that was detached for 3 days, and from a nondetached portion of the retina from the surgical eye. Microglial–immune cells were stained with isolectin. Scale bar, 50 μm. (**B**) Number of lectin-labeled cells per unit area (230 $\times$ 230 μm) of retinal wholemounts obtained from nonsurgical and vitrectomized control eyes and from surgical eyes at 3 and 7 days after surgery. In the case of the surgical eyes, the cell number was determined in the detached retina and in attached retinal areas located in situ near (peridetached) or more distant (10–15 mm) from the detached retina (attached). The vitrectomy control was determined at 3 days after vitrectomy without creation of detachment. The data are expressed as the percentage of the nonsurgical control (100%). The bars represent values obtained in 10 to 24 wholemounts. Significant differences versus nonsurgical control: $^{*}P < 0.05$; $^{**}P < 0.01$; $^{***}P < 0.001$. Significant differences versus vitrectomy control: $^{\bullet}P < 0.01$; $^{\bullet\bullet}P < 0.001$.

Retinal detachment caused a decrease of the plasma membrane K^+ conductance of Müller cells (Figs. 2A–D). The decrease of the K^+ currents was associated with a decrease in the gene and protein expression for the main K^+ channel subtype of Müller cells, Kir4.1 (Fig. 6). In addition, the immunoreactivity for Kir4.1 (but not for Kir2.1) in retinal slices decreased after detachment (Figs. 4A, 4C, 5D). The data suggest that the downregulation of the Kir4.1 protein may represent one if not the main cause of the altered current pattern of Müller cells. Impaired spatial buffering of K^+ ions (normally performed by Müller cells by means of their Kir channels) may contribute to neuronal degeneration in the detached retina, by favoring neuronal hyperexcitation and glutamate toxicity. In the postischemic retina of the rat, it has been shown that the decrease in K^+ currents is associated with altered osmotic swelling characteristics of Müller cells,[35] which may contribute to edema development in the retina.[18] In the detached retina of the pig, the presence of retinal edema both in the extracellular space and within Müller cells has been described previously.[10] However, it remains to be established whether the downregulation of K^+ channel expression in Müller cells contributes to edema in the detached retina. It has been suggested that a decrease in Müller cell K^+ conductance supports the entry of the cells into the proliferation cycle.[36] Whether Müller cells in the detached retina of the pig (similar to cells in detached retinas of other species)[13] proliferate remains to be determined. In addition to the alterations of physiological parameters, gliotic Müller cells in detached retinas showed hypertrophy (Fig. 1) and increased expression of intermediate filaments (Figs. 4A, 4D). By formation of glial scars and cellular hypertrophy, reactive Müller glial cells may inhibit regular neuroregeneration in the detached and reattached retina.

We found that distinct symptoms of Müller cell gliosis were not restricted to the detached retinal areas but occurred also in nondetached retinal regions of the surgical eyes. This involves the increases in intermediate filament expression (Figs. 4A, 4D), the decrease in the whole-cell K^+ currents (Figs. 2A–D) and in the Kir4.1 immunolabeling (Figs. 4A, 5D), and the increase in the incidence of cells that showed Ca^{2+} responses on stimulation of purinergic P2 receptors (Figs. 3B, 3C). In addition, microglial cell activation–immune cell infiltration was observed in both detached and attached tissues (Fig. 7). The decrease of K^+ currents (Fig. 2B) was observed in Müller cells from nondetached areas at 7 but not at 3 days after creation of detachment. However, other indications of retinal gliosis (i.e., microglia proliferation; Fig. 7) and upregulation of GFAP expression (not shown), were already observed at 3 days of detachment. These data may suggest that distinct features of retinal gliosis show a time-dependent spread from the injured into the noninjured surrounding tissue. In addition, we found distinct gradients of changes in the attached retina surrounding the focal detachment for different parameters of glial cell responses (though, in most cases, the differences did not achieve statistical significance): Müller cell hypertrophy (Fig. 1), K^+ currents (Fig. 2C), and immune cell activation (Fig. 7B). The reasons for the presence of gliosis in the nondetached retinal tissue are unclear. Soluble factors such as growth factors and cytokines may diffuse from the detached into the attached

tissue. It has been shown that within minutes of experimental detachment, Müller cells show increased protein phosphorylation (e.g., of the fibroblast growth factor receptor and of the mitogen-activated protein kinases) and increased expression of transcription factors.[8] It is conceivable that, in addition to other factors, endogenously released fibroblast growth factor, which is an inducer of intermediate filament expression in Müller cells[37] diffuses into nondetached retinal areas. Furthermore, ATP, known to evoke long-range Ca^{2+} signaling in the retinal glial cell network and to be released from retinal glial cells on various stimuli (e.g., during mechanical stress[38]), may activate neighboring glial cells. It is noteworthy in this context that stimulation of P2Y receptors has been shown to evoke the release of growth factors from cultured Müller cells.[39]

The increases in the number of isolectin-labeled cells in the nerve fiber layer of retinal wholemounts (Fig. 7) are indicative of microglial cell proliferation and/or immune cell invasion in both detached and attached retinal areas of surgical eyes. The lack of morphologic alterations of these cells after detachment suggests that the immune cell response is mediated predominantly by proliferation of resident microglial cells, because infiltration of immune cells from the blood (which would lack cell processes) appears to be negligible. In support of this assumption, we did not find extravasated albumin immunoreactivity around inner retinal vessels in slices from 7-day detached retinas (not shown), disclosing the presence of vascular leakage at this time. Activated microglial cells are considered one of the most sensitive sensors for pathologic events in the neural tissue, especially in cases of neuroinflammation.[40] Recently, we found that experimental endotoxin-induced uveoretinitis in rats causes a Müller cell reactivity very similar to that observed in the present study (i.e., involving cellular hypertrophy, decrease of K^+ currents, decrease of Kir4.1 protein expression, and upregulation of GFAP expression).[41] Retinal inflammation may represent one factor underlying the spread of the gliotic responses from the detached into the surrounding nondetached retinal areas, and it may be caused by the detachment or even by the surgery alone. However, we found that the vitrectomy procedure per se did not evoke Müller cell gliosis and caused only a slight increase in microglia density (Fig. 7B), which discloses a prominent contribution of the surgery to the glial cell changes. There is another factor that cannot be ruled out as a cause of the gliotic responses in nondetached retinal areas— hypoxia of the inner retina, due to a reduction of the retinal blood flow. It has been shown in patients with rhegmatogenous retinal detachment that the retinal blood flow is reduced in the macular area, even when the macula is not involved[42]; that retinal circulation times of detached areas are longer than those of nondetached areas; and that both are longer than those of normal subjects.[43] Transient ischemia of the rat retina causes Müller cell reactivity very similar to that described in the present study,[35] and it has been shown that hypoxic conditions decrease the gene expression of Kir4.1 in cultured brain astrocytes.[44] Future investigations are necessary to reveal the mechanisms of the spread of gliosis from the detached into the surrounding nondetached tissue.

The causative mechanisms of the elevated Ca^{2+} responsiveness on purinergic receptor stimulation are not fully understood. The immunoreactivities for $P2Y_1$ and $P2Y_2$ receptors are apparently upregulated in the detached tissue compared with the controls (Figs. 4F, 5E). An increased expression of P2Y receptors by Müller cells may explain the increased responsiveness of the cells to ATP. However, in the nondetached tissue, no apparent alteration of the expression of P2Y receptor proteins could be found (Fig. 5E). Therefore, alterations in the functional state of the P2 receptors, or in the coupling of the receptors to Ca^{2+} stores, may contribute to the enhanced responsiveness of Müller cells to ATP observed in the nondetached tissue. This assumption is supported by the recent observation on cultured Müller cells that various growth factors resensitize P2Y receptors, which were depressed in their function by agonist application.[45] It is conceivable that intraretinally released soluble factors may induce the enhanced responsiveness to ATP of Müller cells in nondetached retinal areas. However, alterations in the expression of other subtypes of P2 receptors (not investigated in the present study) cannot be ruled out.

In patients with local retinal detachment, abnormal function can be observed in areas of the visual field that correspond to both detached and nondetached retinal regions.[20,25,26] This observation suggests that, in addition to detached retinal areas, the surrounding nondetached retina undergoes distinct reactive changes. Here, we demonstrate that retinal gliosis is rapidly induced in both detached and attached retinal areas. The gliosis in nondetached retinal areas may reflect, or even may contribute to,[18] neuronal degeneration or remodeling which could explain the impaired recovery of vision in human subjects after reattachment surgery. If this assumption is true, an inhibition of gliosis should exert protective effects,[17] and the application of gliosis-inhibiting factors during reattachment surgery appears as a promising approach that should delay the spread of gliosis into the noninjured tissue and thus support neuroregeneration and optimal recovery of vision after surgery in both the detached and the nondetached retina. Moreover, inhibition of gliosis may prevent the development of proliferative vitreoretinopathy.[46]

Acknowledgments

The authors thank Ute Weinbrecht for excellent technical support.

References

1. Fisher SK, Anderson DH. Cellular effects of detachment on the neural retina and the retinal pigment epithelium. In: Ryan SJ, Wilkinson CP, eds. *Retina.* St. Louis: Mosby; 2001:1961–1986.
2. Cook B, Lewis GP, Fisher SK, Adler R. Apoptotic photoreceptor degeneration in experimental retinal detachment. *Invest Ophthalmol Vis Sci.* 1995;36:990–996.
3. Mervin K, Valter K, Maslim J, Lewis GP, Fisher SK, Stone J. Limiting photoreceptor death and deconstruction during experimental retinal detachment: the value of oxygen supplementation. *Am J Ophthalmol.* 1999;128:155–164.
4. Lewis GP, Linberg KA, Fisher SK. Neurite outgrowth from bipolar and horizontal cells after experimental retinal detachment. *Invest Ophthalmol Vis Sci.* 1998;39:424–434.
5. Faude F, Francke M, Makarov F, et al. Experimental retinal detachment causes widespread and multilayered degeneration in rabbit retina. *J Neurocytol.* 2001;30:379–390.
6. Coblentz FE, Radeke MJ, Lewis GP, Fisher SK. Evidence that ganglion cells react to retinal detachment. *Exp Eye Res.* 2003;76:333–342.
7. Lewis GP, Mervin K, Valter K, et al. Limiting the proliferation and reactivity of retinal Müller cells during experimental retinal detachment: the value of oxygen supplementation. *Am J Ophthalmol.* 1999;128:165–172.
8. Geller SF, Lewis GP, Fisher SK. FGFR1, signaling, and AP-1 expression after retinal detachment: reactive Müller and RPE cells. *Invest Ophthalmol Vis Sci.* 2001;42:1363–1369.
9. Francke M, Faude F, Pannicke T, et al. Electrophysiology of rabbit Müller (glial) cells in experimental retinal detachment and PVR. *Invest Ophthalmol Vis Sci.* 2001;42:1072–1079.
10. Jackson TL, Hillenkamp J, Williamson TH, Clarke KW, Almubarak AI, Marshall J. An experimental model of rhegmatogenous retinal detachment: surgical results and glial cell response. *Invest Ophthalmol Vis Sci.* 2003;44:4026–4034.
11. Uhlmann S, Bringmann A, Uckermann O, et al. Early glial cell reactivity in experimental retinal detachment: effect of suramin. *Invest Ophthalmol Vis Sci.* 2003;44:4114–4122.

12. Anderson DH, Guerin CJ, Erickson PA, Stern WH, Fisher SK. Morphological recovery in the reattached retina. *Invest Ophthalmol Vis Sci*. 1986;27:168–183.
13. Fisher SK, Erickson PA, Lewis GP, Anderson DH. Intraretinal proliferation induced by retinal detachment. *Invest Ophthalmol Vis Sci*. 1991;32:1739–1748.
14. Lewis GP, Guerin CJ, Anderson DH, Matsumoto B, Fisher SK. Rapid changes in the expression of glial cell proteins caused by experimental retinal detachment. *Am J Ophthalmol*. 1994;118:368–376.
15. Marc RE, Murry RF, Fisher SK, Linberg KA, Lewis GP. Amino acid signatures in the detached cat retina. *Invest Ophthalmol Vis Sci*. 1998;39:1694–1702.
16. Newman EA, Reichenbach A. The Müller cell: a functional element of the retina. *Trends Neurosci*. 1996;19:307–312.
17. Fisher SK, Lewis GP. Müller cell and neuronal remodeling in retinal detachment and reattachment and their potential consequences for visual recovery: a review and reconsideration of recent data. *Vision Res*. 2003;43:887–897.
18. Francke M, Faude F, Pannicke T, et al. Glial cell-mediated spread of retinal degeneration during detachment: a hypothesis based upon studies in rabbits. *Vision Res.* 2005;45:2256–2267.
19. Erickson PA, Fisher SK, Anderson DH, Stern WH, Borgula GA. Retinal detachment in the cat: the outer nuclear and outer plexiform layers. *Invest Ophthalmol Vis Sci*. 1983;24:927–942.
20. Chisholm IA, McClure E, Foulds WS. Functional recovery of the retina after retinal detachment. *Trans Ophthalmol Soc UK*. 1975; 95:167–172.
21. Isashiki M, Ohba N. Recovery of differential light sensitivity following surgery for rhegmatogenous retinal detachment. *Graefes Arch Clin Exp Ophthalmol*. 1986;224:184–190.
22. Kroll AJ, Machemer R. Experimental retinal detachment and reattachment in the rhesus monkey: electron microscopic comparison of rods and cones. *Am J Ophthalmol*. 1969;68:58–77.
23. Isernhagen RD, Wilkinson CP. Recovery of visual acuity following the repair of pseudophakic retinal detachment. *Trans Am Ophthalmol Soc*. 1988;86:291–306.
24. Nork TM, Millecchia LL, Stickland BD, Linberg JV, Chao G. Selective loss of blue cones and rods in human retinal detachment. *Arch Ophthalmol*. 1995;113:1066–1073.
25. Sasoh M, Yoshida S, Kuze M, Uji Y. The multifocal electroretinogram in retinal detachment. *Adv Ophthalmol*. 1997;94:239–252.
26. Matsuzaki T, Shinoda K, Inoue M, et al. Multifocal electroretinography after scleral buckling for rhegmatogenous retinal detachment. *Jpn J Ophthalmic Surg*. 2001;14:391–394.
27. Ishii M, Horio Y, Tada Y, et al. Expression and clustered distribution of an inwardly rectifying potassium channel, K_{AB}-2/Kir4.1, on mammalian retinal Müller cell membrane: their regulation by insulin and laminin signals. *J Neurosci*. 1997;17:7725–7735.
28. Nagelhus EA, Veruki ML, Torp R, et al. Aquaporin-4 water channel protein in the rat retina and optic nerve: polarized expression in Müller cells and fibrous astrocytes. *J Neurosci*. 1998;18:2506–2519.
29. Kofuji P, Biedermann B, Siddharthan V, et al. Kir potassium channel subunit expression in retinal glial cells: implications for spatial potassium buffering. *Glia*. 2002;39:292–303.
30. Nagelhus EA, Horio Y, Inanobe A, et al. Immunogold evidence suggests that coupling of K^+ siphoning and water transport in rat retinal Muller cells is mediated by a coenrichment of Kir4.1 and AQP4 in specific membrane domains. *Glia*. 1999;26:47–54.
31. Kofuji P, Ceelen P, Zahs KR, Surbeck LW, Lester HA, Newman EA. Genetic inactivation of an inwardly rectifying potassium channel (Kir4.1 subunit) in mice: phenotypic impact in retina. *J Neurosci*. 2000;20:5733–5740.
32. Uckermann O, Grosche J, Reichenbach A, Bringmann A. ATP-evoked calcium responses of radial glial (Müller) cells in the postnatal rabbit retina. *J Neurosci Res*. 2002;70:209–218.
33. Chandler MJ, Smith PJ, Samuelson DA, MacKay EO. Photoreceptor density of the domestic pig retina. *Vet Ophthalmol*. 1999;2:179–184.
34. Hendrickson A, Hicks D. Distribution and density of medium- and short-wavelength selective cones in the domestic pig retina. *Exp Eye Res*. 2002;74:435–444.
35. Pannicke T, Iandiev I, Uckermann O, et al. A potassium channel-linked mechanism of glial cell swelling in the postischemic retina. *Mol Cell Neurosci*. 2004;26:493–502.
36. Bringmann A, Francke M, Pannicke T, et al. Role of glial K^+ channels in ontogeny and gliosis: a hypothesis based upon studies on Müller cells. *Glia*. 2000;29:35–44.
37. Lewis GP, Erickson PA, Guerin CJ, Anderson DH, Fisher SK. Basic fibroblast growth factor: a potential regulator of proliferation and intermediate filament expression in the retina. *J Neurosci*. 1992; 12:3968–3978.
38. Newman EA. Propagation of intercellular calcium waves in retinal astrocytes and Müller cells. *J Neurosci*. 2001;21:2215–2223.
39. Milenkovic I, Weick M, Wiedemann P, Reichenbach A, Bringmann A. P2Y receptor-mediated stimulation of Müller glial cell DNA synthesis: dependence on EGF and PDGF receptor transactivation. *Invest Ophthalmol Vis Sci*. 2003;44:1211–1220.
40. Kreutzberg GW. Microglia: a sensor for pathological events in the CNS. *Trends Neurosci*. 1996;19:312–318.
41. Pannicke T, Uckermann O, Iandiev I, Wiedemann P, Reichenbach A, Bringmann A. Ocular inflammation alters swelling and membrane characteristics of rat Müller glial cells. *J Neuroimmunol*. 2005;161:145–154.
42. Eshita T, Shinoda K, Kimura I, et al. Retinal blood flow in the macular area before and after scleral buckling procedures for rhegmatogenous retinal detachment without macular involvement. *Jpn J Ophthalmol*. 2004;48:358–363.
43. Satoh Y. Retinal circulation in rhegmatogenous retinal detachment demonstrated by videofluorescence angiography and image analysis, I: the condition of retinal circulation before retinal detachment surgery (in Japanese). *Nippon Ganka Gakkai Zasshi*. 1989;93: 1002–1008.
44. Li L, Head V, Timpe LC. Identification of an inward rectifier potassium channel gene expressed in mouse cortical astrocytes. *Glia*. 2001;33:57–71.
45. Weick M, Wiedemann P, Reichenbach A, Bringmann A. Resensitization of P2Y receptors by growth factor-mediated activation of the phosphatidylinositol-3 kinase in retinal glial cells. *Invest Ophthalmol Vis Sci*. 2005;46:1525–1532.
46. Asaria RH, Kon CH, Bunce C, et al. Adjuvant 5-fluorouracil and heparin prevents proliferative vitreoretinopathy: results from a randomized, double-blind, controlled clinical trial. *Ophthalmology*. 2001;108:1179–1183.